European Journal of Pharmaceutics and Biopharmaceutics 172 (2022) 144–156

Contents lists available at ScienceDirect

European Journal of Pharmaceutics and Biopharmaceutics

journal homepage: www.elsevier.com/locate/ejpb

Lactoferrin-loaded nanostructured lipid carriers (NLCs) as a new formulation for optimized ocular drug delivery

Rubén Varela-Fernández [a,b], Xurxo García-Otero [a,c], Victoria Díaz-Tomé [a], Uxía Regueiro [b], Maite López-López [b], Miguel González-Barcia [d], María Isabel Lema [e,*], Francisco Javier Otero-Espinar [a,f,g,*]

[a] Department of Pharmacology, Pharmacy and Pharmaceutical Technology. University of Santiago de Compostela (USC), Campus vida. Santiago de Compostela. Zip Code: 15782, Spain
[b] Clinical Neurosciences Group, University Clinical Hospital, Health Research Institute of Santiago de Compostela (IDIS), Travesía da Choupana s/n Santiago de Compostela. Zip Code: 15706, Spain
[c] Molecular Imaging Group, University Clinical Hospital, Health Research Institute of Santiago de Compostela (IDIS), Travesía da Choupana s/n Santiago de Compostela. Zip Code: 15706, Spain
[d] Clinical Pharmacology Group, University Clinical Hospital, Health Research Institute of Santiago de Compostela (IDIS), Travesía da Choupana s/n Santiago de Compostela. Zip Code: 15706, Spain
[e] Department of Surgery and Medical-Surgical Specialties, Ophthalmology Area. University of Santiago de Compostela (USC), Campus Vida. Santiago de Compostela. Zip Code: 15706, Spain
[f] Paraquasil Group. University Clinical Hospital, Health Research Institute of Santiago de Compostela (IDIS), Travesía da Choupana s/n Santiago de Compostela. Zip Code: 15706, Spain
[g] Institute of Materials iMATUS. University of Santiago de Compostela (USC), Campus vida. Santiago de Compostela. Zip Code: 15782, Spain.

ARTICLE INFO

Keywords:
Nanostructured lipid carriers (NLC)
Double emulsification-solvent evaporation method
Lactoferrin
Ocular drug delivery
Topical ophthalmic administration
Keratoconus

ABSTRACT

Nanostructured lipid carriers (NLC) are novel lipidic nanosystems that provide significant improvements in terms of high drug loading capacity and controlled drug release. The purpose of the present work was based on the design, development, and physicochemical characterization of lactoferrin-loaded NLCs as a new therapeutic alternative for the keratoconus treatment. Lactoferrin-loaded NLCs were successfully prepared by a double emulsion/solvent evaporation method. The resultant NLC were assessed in terms of particle size, size distribution, surface charge, morphology, encapsulation efficiency (EE), loading capacity (LC), stability, cytotoxicity, *in vitro* release, and ocular surface retention. Resulting data showed a size of 119.45 ± 11.44 nm, a 0.151 ± 0.045 PDI value and a surface charge of −17.50 ± 2.53 mV. Besides, high EE and LC values were obtained (up to 75%). The *in vitro* release study demonstrated a lactoferrin controlled release pattern. NLCs were also stable, non-toxic and show mucoadhesive properties. Thus, a consistent preclinical base was obtained, where NLC may be considered as a potential controlled release novel drug delivery system of lactoferrin for the keratoconus treatment.

1. Introduction

The eye is one of the daintiest, highly protected, and complex organs, with distinctive structure, composition, and biochemistry. In contrast to the conventional systemic drug delivery pathways, topical ophthalmic administration is a non-invasive and the most favored pathway for drug delivery, particularly to the anterior segment of the eye. Nevertheless, the ocular bioavailability of the active substances may be very low due to the different barriers that may hinder the drug transport and its subsequent low residence time at the target site. Hence, an idyllic drug delivery system (DDS) that effectively ranges the target site without disturbing the ocular structural barriers is needed [1–4].

NLC have shown great promise properties (e.g., drug protection, enhanced bioavailability, dose reduction, or prolonged circulation time, among others) as controlled DDS in the recent years [5,6]. Nanoparticulate lipidic DDS have reached enough interest in the recent years,

* Corresponding authors.
E-mail addresses: xurxo.garcia.otero@gmail.com (X. García-Otero), miguel.gonzalez.barcia@sergas.es (M. González-Barcia), mariaisabel.lema@usc.es (M. Isabel Lema), francisco.otero@usc.es (F. Javier Otero-Espinar).

https://doi.org/10.1016/j.ejpb.2022.02.010
Received 29 December 2021; Received in revised form 2 February 2022; Accepted 14 February 2022
Available online 17 February 2022

predominantly due to their biocompatibility with the ocular surface, as well as to their lipophilicity and capability of permeating physiological barriers. Other properties, such as simplicity in the elaboration method, cost-effectiveness ratio and the practicability of large-scale manufacture, turn them into attractive and marketable drug delivery alternatives to the anterior segment of the eye [7,8].

NLC are a novel generation of lipid nano-sized systems which were designed to surpass the drawbacks of previously developed lipidic colloidal systems (liposomes, solid lipid nanoparticles, …). NLC exist as a solid lipid matrix at body and room temperature, where a percentage is changed for a mixture of liquid lipids, resulting in a less ordered lipid matrix. NLC formulations were deeply studied due to their potential as ocular DDS to enhance corneal permeation and improve the drug bioavailability, as well as safety, non-invasive and improve patient's compliance [1,9]. Moreover, the mucoadhesive nature of NLC improves their contact with the eye surface, leading to a sustained residence time, greater bioavailability and reduced side effects [10]. NLC have also shown high drug encapsulation and loading efficiencies for both lipophilic and hydrophilic drugs [11,12], long shelf-life and large scale production [13–16].

Keratoconus (KC) is a degenerative ecstatic corneal disorder with a progressive bilateral pattern that mainly appears in young adults, leading to pronounced visual disability, deteriorating over time [17]. Currently, there is no available treatment related to the prevention of the development or progression delay of this disease. Moreover, the palliative care does not curb the progression of the ecstatic disorder; invasive surgical procedures are used as the ultimate alternative, preferably intracorneal ring segments (ICRS) implantation, corneal transplant, or corneal cross linking (CXL), with incomplete visual upturn [18,19]. The etiology and its progression determinants are still unclear despite its high prevalence, although a multi-factorial pattern is dilucidated, as the last common trail of several pathological processes [20].

Keratoconus progression is related to a gradual increase of inflammatory intermediaries, comprising cytokines and cell adhesion glycoproteins. Certainly, different studies have proven the correlation between the overexpression of Tumor Necrosis Factor α (TNF-α), Interleukin-6 (IL-6), and Matrix-9-Metalloprotease (MMP-9) was described as a key factor in the KC progression [21,22]. Additionally, a noteworthy diminution in lactoferrin lacrimal levels, as well as other glycoproteins, was also noticed in the KC pathogenesis [23,24]. These findings may indicate that immunological courses may be related to the appearance and development of this corneal ectasia.

Lactoferrin (Lf) is a globular protein (two homologous globular N- and C- lobes) with iron-binding capacity [25,26], as well as different biological effects, including anti-inflammatory [27,28], antibacterial [29–31], antiviral [32–34] and antitumoral [35,36], among others. Consequently, the use of Lf in different surface ocular pathologies as Sjögren syndrome, idiopathic dry eye, vernal, irritative or giant papillary conjunctivitis, keratoconjunctivitis, bacterial and viral ocular infections has been previously proposed [37]. Additionally, this protein has also proven to modulate the humoral and cellular response involving Toll-Like receptors (TLRs) and to stimulate the corneal wound healing [37–39]. A TLR 2–4 receptors overexpression, an increase in pro-inflammatory cytokines and a Lf lacrimal levels decrease in granulocytes of keratoconus patients were previously demonstrated by our group [40–42]. These and other evidences indicate that Lf may also have an important role in the keratoconus treatment [22–24].

The aim of the present work was grounded on the design, development, and characterization of Lf-loaded NLCs as nanosized systems intended for the topical ophthalmic treatment including KC. Similarly, the central commitment of this site-specific and controlled-delivery approach is predominantly centered on the understanding of enhanced pharmacokinetics and pharmacodynamics drug properties, together with better immunogenicity to improve the therapeutic effect. An effort to prove the appropriateness of NLC to control the Lf release and improve its corneal permeability was also studied by acquiring a strong preclinical foundation. Indeed, a new ocular biopermanence assay based on a radiolabeling method was performed to evaluate the NLC bioadhesion proposed for topical instillation.

2. Materials

Glycerol monostearate 40–55 was purchased from Roig Farma S.A. (Barcelona, Spain). Soy lecithin was acquired from Acofarma® (Barcelona, Spain). Cholesterol from lanolin was provided by Sigma Aldrich Chemie GmbH (St Louis, USA). Compritol 888 ATO (a mixture of mono-, di- and triglycerides of behenic acid (C22)) and Capryol® 90 (propylene glycol monocaprylate) were generously presented by Gattefosse (Paris, France). Miglyol® 812 N (medium-chain triglycerides) was kindly donated by IOI Oleochemical GmbH (Witten, Germany). Poloxamer 407 (Kolliphor® P 407), Poloxamer 188 (Kolliphor® P 188) and D-α-Tocopherol Polyethylene Glycol 1000 Succinate were supplied by Sigma Aldrich Chemie GmbH (St Louis, USA). Lactoferrin was acquired from Sigma-Aldrich (St Louis, USA). All supplementary elements and reagents were of the uppermost available pureness score.

3. Methods

3.1. Preparation of lactoferrin-loaded NLC

Lf-loaded NLC were obtained by a customized double emulsion/solvent evaporation technique (DE/SE) (see details of the NLC composition in Table 1). Briefly, the mixture of solid and liquid lipids was dissolved in 5 mL dichloromethane (organic phase). Inner aqueous phase (W1) was prepared by dissolving predetermined amounts of Lf in PBS, containing a 30% (w/v) Kolliphor® P407. The first emulsion was obtained by emulsification of the aqueous phase with the organic phase in a 1:5 (v/v) ratio by sonication (Bandelin Sonoplus® HD3200, Germany) at 15% sonication amplitude for 2 min (pulse: 30 s – 5 s). The second emulsion (W2) was obtained by adding the first emulsion to an α-Tocopherol PEG aqueous solution in a 1:10 (v/v) ratio by sonication at 20% sonication amplitude for 5 min (pulse: 30 s – 5 s). The organic solvent in the double emulsion was evaporated during the sonication process. Double emulsion was then included into a maturation medium, composed of a 0.5% (w/v) Kolliphor® P188 aqueous solution (included into an ice-bath) for 3 h under magnetic stirring (100 rpm). Resulting NLC were then filtered through a 0.8 mm cellulose acetate filter and subsequently ultracentrifugated at 50000 rpm and 25 °C for 1 h (TL-100 Ultracentrifuge, Beckman Coulter). The final NLC concentrate was resuspended in Milli-Q® water, examined and subsequently lyophilized. The supernatant was retrieved for additional studies.

3.2. Physicochemical characterization of lactoferrin-loaded NLC

3.2.1. Particle size, size distribution and ζ potential

Particle size and size distribution are crucial characteristics due to their influence on the final formulation properties (stability, solubility, release rate or biological behavior, among others). The average size, PDI and surface charge of the NLCs were determined by dynamic light scattering (DLS) with non-invasive back scattering (DLS-NIBS) at 25 °C (ZEN3600, Malvern Instruments Ltd., UK). Sample preparation was described in previous works [43]. Each batch was tested in triplicate.

3.2.2. Morphological evaluation

Morphology denotes the outer features of nanoparticles. NLC are presumably anisometric particles (high surface area), where oil droplets are included between the solid platelets and the surfactant layer [44]. In addition, particle morphology significantly influences a lot of physicochemical characteristics, such as the encapsulation efficiency, loading capacity, drug release, pharmacokinetics, biodistribution or cellular uptake, among others [45,46].

The NLC morphological examination was carried out by Scanning

Table 1
Composition of the previously optimized Lf-loaded NLC formulation.

Solid lipid		Liquid lipid		Surfactant	
Name	*Ratio (w/v)*	*Name*	*Ratio (w/v)*	*Name*	*Ratio (w/v)*
Glycerol monostearate	12%	Capryol® 90	15%	Kolliphor® P 407	30%
Compritol® 888 ATO	12%	Miglyol® 812 N	45%	Kolliphor® P 188	0.5%
Soy lecithin	12–30%			α-Tocopherol-PEG	0.5%
Cholesterol	5–7.5%				

Electron Microscopy (SEM) and Transmission Electron Microscopy (TEM), as previously described [43]. Briefly, SEM analysis were carried out by positioning the freeze-dried NLCs on a metal specific holder and iridium coating was further applied preceding the microscopical analysis under different magnifications. An appropriate preparation procedure was also performed over the samples prior to TEM analysis (JEM-F200CF-HR microscope) by dyeing formulations with a 2% (w/v) phosphotungstic acid aqueous solution and ulterior all-night drying.

3.2.3. Determination of production yield, encapsulation efficiency and loading capacity

The production yield (PY) of the resulting NLC was obtained by the centrifugation procedure [47], with negligeable changes. Briefly, fixed NLCs volumes were ultracentrifuged at 50000 rpm and 25 °C for an 1 h. Ultracentrifugation led the NLC concentration in the surface of the suspension. Aqueous residue was then discarded, and the concentrated NLC were finally freeze-dried. The PY was then estimated as presented:

$$Productionyield(\%) = \frac{Nanoparticlesweight}{Totalinitialsolidsweight}\hat{A}\cdot 100$$

Encapsulation efficiency (EE) and loading capacity (LC) of NLCs were obtained after separation by centrifugation, as previously described (see section 3.1.). The amount of boundless Lf was measured in the resulting aqueous residue by UV–Vis spectrophotometry (λ = 280.0 nm). EE and LC were finally estimated as presented below:

$$EE(\%) = \frac{Totalamountofdrug - Amountofunbounddrug}{Totalamountofdrug}\hat{A}\cdot 100$$

$$LC(\%) = \frac{Totalamountofdrug - Amountofunbounddrug}{Nanoparticlesweight}\hat{A}\cdot 100$$

3.3. Stability studies

Several colloidal structures (micelles, liposomes or nanoemulsions) included into the NLC formulations may have an important impact on the NLC stability. Aggregation or coagulation phenomena may arise because of collisions among particles, leading to caking or flocculation throughout long-term stability [48].

3.3.1. Stability to storage

The stability-to-storage assay was planned according to the ICH guidelines [49], with negligeable adjustments. Resulting NLC formulations were freshly prepared, contemplating size changes and probable aggregation phenomena. Three different temperature subsets were established for the NLC incubation (4 °C, 25 °C, and 37 °C for an 8 h and 3-month period for short and long-term stability respectively, under magnetic stirring, protected from light. Samples were taken at predefined intervals for particle size and distribution determination, carrying out every measurement in triplicate.

3.3.2. Stability to pH

The NLC stability assessment to pH changes was performed in newly prepared formulations. NLC were preserved at 4 ± 2 °C as standard formulations. A prefixed volume of each NLC suspension (500 μL) was included and diluted to a final volume using double-distilled water (5 mL). pH was subsequently changed to prearranged values (from 2 to 12). Resulting formulations were preserved in cooling temperature for 1 day, prior to the measurement by DLS analysis. Each sample was triplicate measured.

3.3.3. Stability to ionic strength

Newly prepared NLC formulations were subjected to ionic strength changes to complete the assessment of their physical stability. NLC were preserved at 4 ± 2 °C as standard formulations. A prefixed volume of each NLC suspension (500 μL) was included into a final volume using double-distilled water (5 mL). The ionic concentration was subsequently changed to prearranged values (from 0.2 to 2.0 M). Resulting formulations were preserved in cooling temperature for 1 day, prior to the measurement by DLS analysis. Each sample was measured thrice.

3.4. In vitro release study

The dialysis method is commonly used to quantify the drug release from nanosized systems. In the present system, two compartments are divided by a dialysis membrane, as previously described [43], building an appropriate system to evaluate the drug release behavior from different types of DDS [50–52].

The Lf release from NLC was evaluated to forecast the drug diffusion and kinetic profile from the delivery systems. The Lf release rate from NLC was measured by UV–Vis spectrophotometry, using Franz diffusion cells. The assembly, filling and conditioning process was explained in detail in previous works [43]. The assay was performed for a 1-day period, and NLCs were tested in triplicate. The diffused protein was finally measured by UV–Vis spectrophotometry at a 280.0 nm wavelength. Analytic validation was previously obtained by our group and showed linearity (R = 0.999) over a concentration interval of 0.4882 – 500 μg/mL and LOD and LOQ values of 0.9765 μg/mL and 1.9531 μg/mL, respectively (data not published). Results proved that NLCs remained stable for at least 7 days, sheltered from light and under cooling.

3.5. Ophthalmic toxicity analysis

The achievement in planning and creating alternative experiments to swap the Draize test has persisted slippery because of the complications of matching the *in vitro* outcomes and animal information. The alternative approaches encompass organotypic models, whose effectiveness was well proven for specific and limited purposes [53–55].

The Bovine Corneal Opacity and Permeability test (BCOP) is an appropriate assay for the evaluation of mild, moderate, and severe ocular irritants. Nonetheless, the BCOP steadfastness is limited for mild irritancy levels. Henceforth, BCOP may be contemplated as a prevalidation test, whose results can be used in combination with alternative irritancy tests, such as the Hen's Egg Test on the Chorioallantoic Membrane assay (HET-CAM) assay [56–59]. In turn, the HET-CAM test is also contemplated a suitable template for modelling the consequences of materials on ocular tissues [55].

3.5.1. Bovine corneal opacity and permeability test (BCOP)

The BCOP is an organ-like trial that permits the appraisal of the hypothetical ocular irritancy of formulations, safeguarding the animal

replacement compliance. A complete scan of all corneal layers can be performed by using *in situ* isolated corneas, enabling the assessment of accurate quantifiable endpoints.

The BCOP basis were previously described by Tchao et al. (1988) [60] and improved by Gautheron et al. [61], with negligeable variations. The assembly, conditioning, application procedure of the formulations and opacity measurements were explained in detail in previous works [43]. Briefly, BCOP test was carried out by using fresh bovine corneas obtained from a local slaughterhouse (Compostelana de Carnes S.L., Santiago de Compostela). The initial corneal opacity was firstly determined by luxmetry and UV–Vis spectrophotometry, taking into account the corneal blank values prior to measurement determination to remove background light exposure. Second, 1 mL PBS was added into the Franz cell's donor chamber, followed by cornea's incubation for 60 min and subsequently opacity determination. Third, 1 mL formulation was incorporated into the upper compartment for 10 min, trailed by its removal and posterior PBS addition for 2 h; the opacity establishment was then made again. Finally, the permeability assessment was furtherly quantified by adding a prefixed volume of a 0.4% (w/v) fluorescein solution (1 mL) to the donor chamber for 90 min and subsequently assessing the PBS optical density (OD) in the receptor compartment at 490.0 nm to estimate the potential corneal permeability variations. The resulting data were finally used to estimate the so-called *in vitro* irritation score (IVIS) [61,62], by applying the following mathematical equation:

$$IVIS = meanopacityvalue + (15 \times meanpermeabilityOD_{490}value)$$

3.5.2. Hen's egg test on the chorioallantoic membrane (HET-CAM)

The HET-CAM test is one of the most common organotypic models used for the identification of irritative compounds, as an alternative to the standard Draize test [63]. In this test, three potential consequences were determined (hemorrhage, lysis and coagulation) and subsequently quantified by means of an irritation score (IS), considering the Kalweit et al. criteria [64]. All practices with eggs were trailed by the appropriate principles and techniques for management of animal supplies.

The procedure was adjusted from the guidelines formerly developed by Spielmann and Liebsch [65], with minor modifications. The assembly, conditioning, application procedure of the formulations and irritancy measurements were explained in detail in previous works [43]. Each NLC suspension was evaluated in triplicate.

3.6. Ocular surface retention study

3.6.1. Ex vivo ocular surface retention study

The protocol previously developed by Belgamwar et al, (2009) and Gradauer et al, (2012) was taken as a reference to perform the *ex vivo* corneal surface retention study [66,67], with negligible changes. Thereby, newly removed eyes were obtained from a home-grown abattoir, macroscopically inspected and feasible ones were chosen for additional exploration. Excised eyes were placed on individual containers, with the corneal surface up. Then, a prefixed volume of a 0.4% (w/v) fluorescein stained NLC suspension (500 μL) were instilled, repeating this process ten times. The residual NLC suspension was measured at a 490.0 nm wavelength by UV–Vis spectrophotometry in order to determine the fluorescence intensity. Each formulation was tested in triplicate. The NLC mucoadhesion data was finally quantified as presented:

$$Mucoadhesion(\%) = \frac{(Initialabsorbance - Initialvolume) - (Finalabsorbance - Finalvolume)}{(Initialabsorbance - Initialvolume)} \hat{A} \cdot 100$$

3.6.2. In vivo ocular surface retention assay

3.6.2.1. Radiolabeling stability and efficiency of NLC. Radioactive fluoride (^{18}F) is one of the most employed positron emitter because of its ideal positron properties ($t_{1/2} = 109.7$ min, $E_{\beta+,max} = 635$ keV, and β^+ intensity = 97%). In recent years, a series of approaches were studied to trace nanosized systems using the 2-[^{18}F]-fluoro-2-deoxy-D-glucose (^{18}F-FDG) labeling technique [68–71]. The experimental procedure for the labeling of NLCs and the subsequent assessment of the labeling efficiency was already detailed in previous works [43].

The NLC radiolabeling efficiency was evaluated by the ^{18}F-FDG activity measurement, together in the supernatant (containing the NLC) and the aqueous residue, in view of the maturation period, as well as the radiotracer disintegration. Finally, a mathematical treatment was applied to the subsequent results to calculate the radiolabeling efficiency and to evaluate the labeling stability over time.

3.6.2.2. In vivo evaluation of the ocular biopermanence. The NLC's biopermanence was executed by Positron Emission Tomography (PET) and Computed Tomography (CT) combined procedure. Both approaches were described in previous works in order to guide the radiolabeling and the successive quantitative biopermanence assessment of new DDS intended for topical ophthalmic administration [43,72].

The *in vivo* studies were performed on male rats, provided by the university's animal-housing unit. The animals were firstly acclimatized and maintained in separate containers under precise environmental and feeding conditions. All animals were manipulated taking into account the ARVO frameworks, together with the standard guidelines for laboratory animals [73]. NLC were analyzed in quadruplicate to undertake the 3Rs governing outlines [74]. The assembly, conditioning, application procedure of the formulations and the measurements of the *in vivo* ocular biopermanence were explained in detail in previous works [43]. The GraphPad Prism® and pKSolver® software were used to establish the appropriate correlation fitting between the remaining formulation activity and time into a single exponential decay equation by means of a single compartment prototype [75]. Non-compartmental approach was additionally performed by approximating the mean residence time (MRT) and the total area under the curve (AUC) of the NLC remaining percentage versus time.

4. Results and discussion

4.1. Preparation of lactoferrin-loaded NLC

The choice of an adequate technique for the NLC elaboration is highly dependent on the drug physicochemical characteristics. A great variety of methods were successfully developed for the incorporation of hydrophobic compounds into the NLC, but there are hardly any described methods for the encapsulation of hydrophilic drugs (e.g., proteins) into NLC, due to the difficulties involved (drugs with high hydrophilicity are significantly ejected from the hydrophobic matrix into the dispersing aqueous phase) [76–79]. Nevertheless, the DE/SE preparation method, where the first emulsion acts as a reservoir, is typically employed to encapsulate hydrophilic drugs, whereas the second emulsion serves as a diffusion barrier, preventing drug leakage from internal to external aqueous phase.

Initial screening studies were carried out to assess the formulation and processing parameters of the NLC preparation procedure. Drug:lipid ratio, oil:aqueous phase ratio, surfactant concentration, volume of the maturation medium, and sonication time were identified as critical factors in producing stable formulations. The results from the initial screening trials (data not shown) suggested that specific values of these parameters are required in the obtention of NLC.

Likewise, colloidal systems involve small particle size and narrow size distribution for high stability and low ocular toxicity [13]. Optimized NLC formulations were in the nanometric range, as a unimodal population with a relatively narrow size distribution, and negatively charged surface. These are several of the most important prerequisites for ocular application of nanoparticulate systems [80].

4.2. Physicochemical characterization of NLC

4.2.1. Particle size, size distribution and surface charge

The NLC traditional diameter varies from 10 to 1000 nm, although a 50–300 nm size interval is especially desired for site-specific drug release [13]. A higher barrier permeability, improved uptake, rapid action, and controlled release are one of the most important advantages of these lipid nanocarriers.

The average size of both blank and lactoferrin-loaded NLC was below 150 nm (see Table 2). The PDI was found to be lower than 0.3, denoting a relative uniformity in the final NLC suspension. The NLC surface charge revealed high negative values (-18.25 ± 2.20 and −17.98 ± 2.54 for blank and lactoferrin-loaded NLC, respectively), being attributed to the chemical nature of the lipid matrix and the surfactants included into the maturation medium (Kolliphor® P188).

Moreover, at lower amounts of lipids, the ability of surfactant to stabilize particles could be enhanced [81]. Surfactant amount also had a significant effect on PDI that could feasibly be associated with the lower predisposition to form aggregates [82,83]. Even though, surfactants proportion in the optimized NLC formulations may stabilize the system without causing an increase in the PDI values.

4.2.2. Morphological evaluation

The TEM analysis offered evidence about the NLC's particle size and morphology and confirmed previous DLS data, where a size below 200 nm was found for the final NLC. Further, the microstructural analysis confirmed that NLC were mostly composed of a uniform population of anisometric, spherical in shape and well-defined size particles (see Fig. 1).

TEM images also showed the nanocapsular structure of the NLC where a less dense non-lipid core corresponding to the aqueous gelled core was observed, as well as a denser external lipid layer. The presence of the aqueous core is very important for the immobilization of lactoferrin since its hydrophilic nature prevents the glycoprotein dispersion to the lipid layer.

SEM analysis demonstrated that the NLC external characteristics were maintained after the elaboration process. SEM analysis also proved the presence of a population of anisometric particles (see Fig. 1). Accordingly, the lyophilized NLC suspensions guaranteed the nanoscale size, being these results aligned with the TEM morphological evaluation. To point out, it must be considered that the NLC's irregular shape observed in SEM images could be caused by the water extraction from the NLC core as consequence of the lyophilization process (see Fig. 2).

4.2.3. Production yield, encapsulation efficiency and loading capacity of NLC

Fig. 3 shows the PY, EE and LC data of the final Lf-loaded NLC. The EE assessment confirmed that the preparation process of the Lf-loaded NLC was reproducible and efficient with PY values above 78.92 ± 9.12% for the optimized lactoferrin-loaded NLC (C_{Lf} = 1 mg/mL) (see Table 2). A correlation in the EE and LC data was perceived with the proportional Lf increase into the NLC suspension (see section 4.2.4). It must be considered that the drug:lipid ratio varied from 1:7.5 to 1:45, reaching high values of EE and LC (up to 75%) for a 1 mg/mL lactoferrin concentration, as presented in Fig. 3 (see section 4.2.4).

4.2.4. Effect of protein loading on size, EE, and LC

Fig. 3 displays the Lf loading effect on size, EE, and LC for Lf-loaded NLC over the increased amount of Lf (from 0.1 to 1.0 mg/mL). Resulting data suggest that Lf amount has a negligeable effect on particle size, although it must be considered that the drug:lipid ratio ranged from 1:7.5 to 1:45, so that the influence may be masked by the large amount of lipidic components. Nevertheless, a correlation in the EE and LC data was found over the increased Lf amount (from 0.1 to 1 mg/mL), although no difference was found in terms of size increase.

Resulting data was subsequently evaluated by a one-way ANOVA analysis, where differences among the Lf-loaded NLC might be observed. EE (%) and LC (%) data were found to be significantly different between NLC formulations ($F = 124.7$, $P < 0.0001$ for EE and $F = 175.4$, $P < 0.0001$ for LC). These results suggest that NLCs might further encapsulate the drug into their matrix, leading to high drug uptake.

These results showed that NLCs have a greater ability to immobilize Lf than previously developed chitosan-based nanoparticles [43]. In this previous study, a consistent preclinical base was obtained by our group based on the design, development, and characterization of chitosan-based NPs to immobilize and promote a controlled release of Lf. Certainly, the ability of chitosan/tripolyphosphate nanoparticles (CS/TPP NPs) and chitosan/sulfobutylether-β-cyclodextrin nanoparticles (CS/SBE-β-CD NPs) to immobilize and release Lf was studied. In this previous research, EE values of 47.19 ± 2.97% and 52.84 ± 1.05% and LC values of 43.47 ± 5.04% and 43.44 ± 3.69% for CS/TPP and CS/SBE-β-CD NPs were obtained for a 1 mg/mL [43]. Nevertheless, these results were lower than those obtained for the present NLC formulations, which showed values greater than 75% for the same Lf concentration. The high immobilization capacity of NLCs could be explained by its nanocapsule structure. The presence of the aqueous polymeric reservoir in the core improves the immobilization of lactoferrin, that can also be adsorbed to the surface of the external lipid layer.

4.3. Stability studies

The physical stability of NLC dispersions is one of key product characteristics to be assessed. NLC formulations are usually heterogeneous and thermodynamically unstable systems. Hence, a noteworthy predisposition to lose physical stability during storage is presumably observed in this type of formulations [84], although the use of an optimized stabilizer composition may maintain the physical stability for several years [85].

Table 2
Particle size, polydispersity index, and surface charge of blank and Lf-loaded NLC formulations. Results are represented as the mean ± S.D. (n = 3).

Formulation	[Lf] (mg/mL)	Size (nm)	PDI	ς Potential (mV)
Blank NLC	–	115.97 ± 15.58	0.152 ± 0.037	−18.25 ± 2.20
Lactoferrin-loaded NLC	0.1	117.91 ± 12.90	0.146 ± 0.042	−18.57 ± 2.47
	0.5	123.09 ± 8.29	0.165 ± 0.040	−17.86 ± 1.51
	1.0	119.45 ± 11.44	0.151 ± 0.045	−17.50 ± 2.53

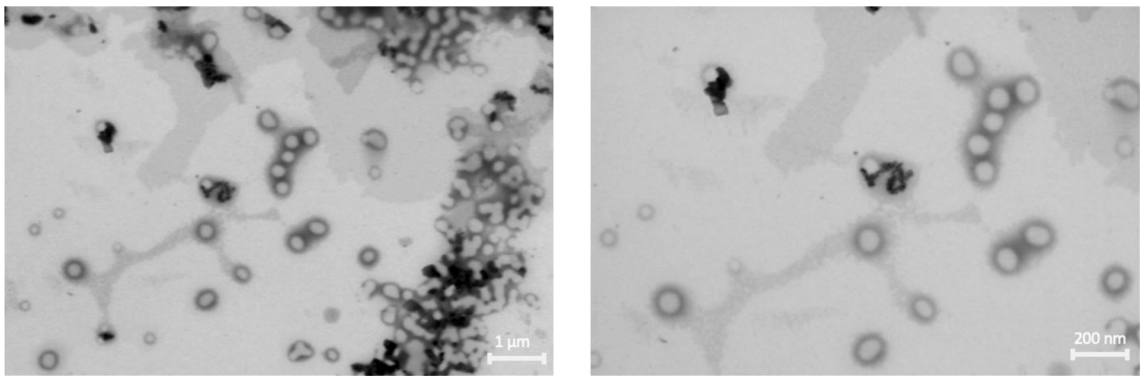

Fig. 1. TEM micrographs of Lf-loaded NLC.

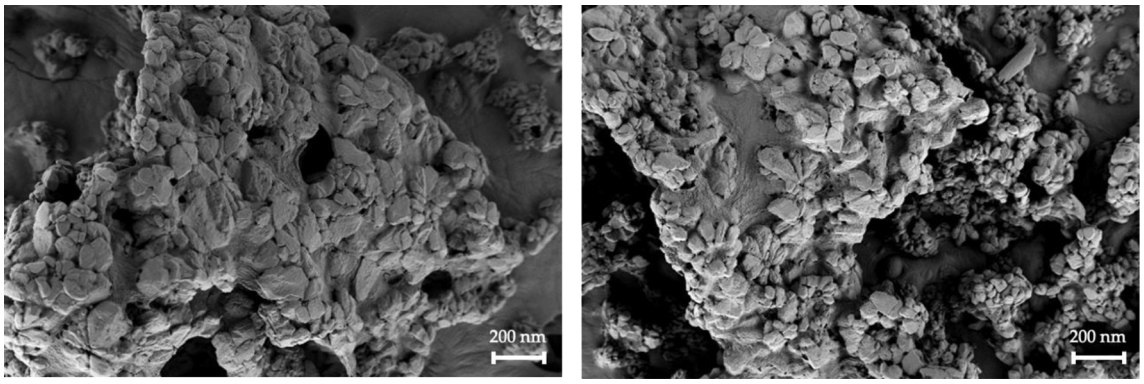

Fig. 2. SEM images of lactoferrin-loaded NLC formulations.

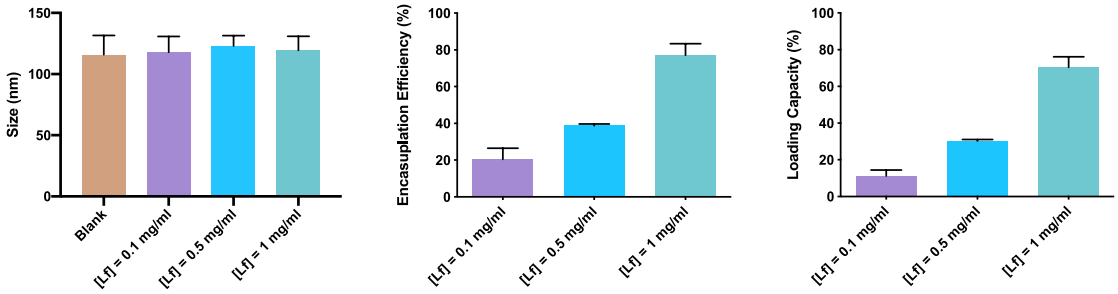

Fig. 3. Evolution of size (nm) and ζ potential (mV), as well as EE (%) and LC (%) values, over increased lactoferrin concentration for NLC formulations.

4.3.1. Stability to storage

The NLC's stability study was carried out by measuring the size, PDI and ς potential at three different temperature sets (see section 3.3.1.) for two different periods (8 h and 3 months, for short and long-term stability study, respectively) (see Fig. 4). Resulting data for both stability studies proved that NLCs were stable in terms of size and size distribution along the studied periods. A one-way ANOVA analysis was finally employed, and no differences (p greater than 0.05) were spotted along the predefined interval, agreeing with the experimental results.

4.3.2. Stability to pH

Fig. 5 shows particle size and surface charge variations of NLC formulations for the tested pH interval. Changes along the studied pH interval are presumably associated with the composition of the resulting formulation, where both solid and liquid lipids determine the nanocarrier's surface charge. Hence, aggregation phenomena were detected in the lower acidic pH interval (from pH 2 to 4), because of the interaction between the acidic media (high proton concentration) and the negatively charged groups of the lipid nanocarriers, neutralizes the nanoparticle's surface charge (ζ potential ≈ 0). Nevertheless, from a pH 6 value, NLC remained stable in size, where high negatively ζ potential values were also observed, supporting these results. Thus, NLC would be suitable for topical ophthalmic administration without producing corneal injuries or lacrimation (pH interval: from 4 to 8) [86].

4.3.3. Stability to ionic strength

The collapse, rupture, or coalescence of the NLC may be associated with modifications in the ionic concentration of the media. This report is reinforced by the electrical double-layer theory, where increasing ionic strength values are associated with a decrease in the double layer thickness [87]. Therefore, an upsurge in the contact between particles may produce an intensification in the NLC's aggregation.

The time-dependent caking, flocculation or deposition phenomena may occur on NLC suspensions due to changes on ionic strength of the

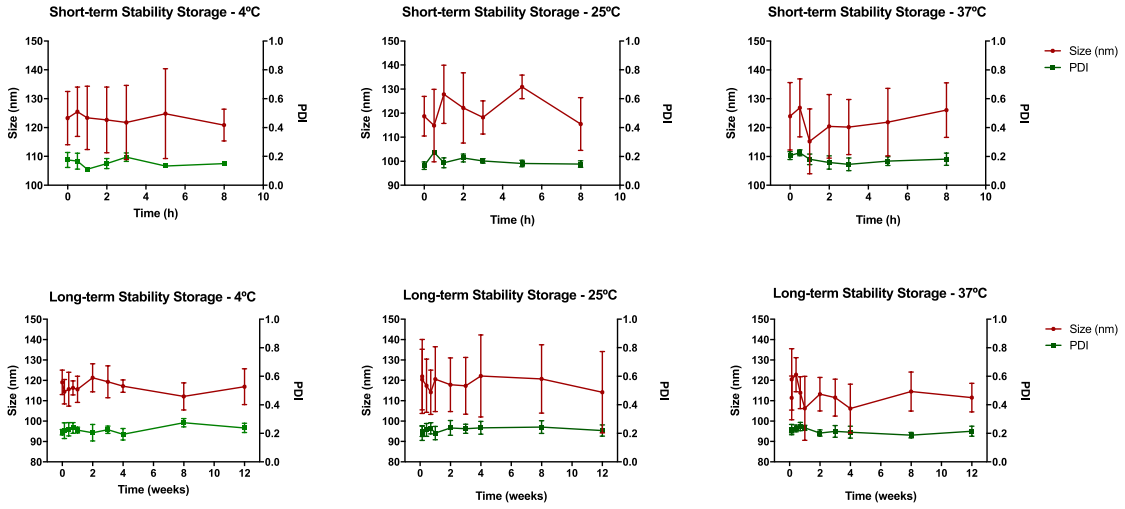

Fig. 4. Short-term (8-hour period) and long-term (3-month period) stability-to-storage study for lactoferrin-loaded NLC.

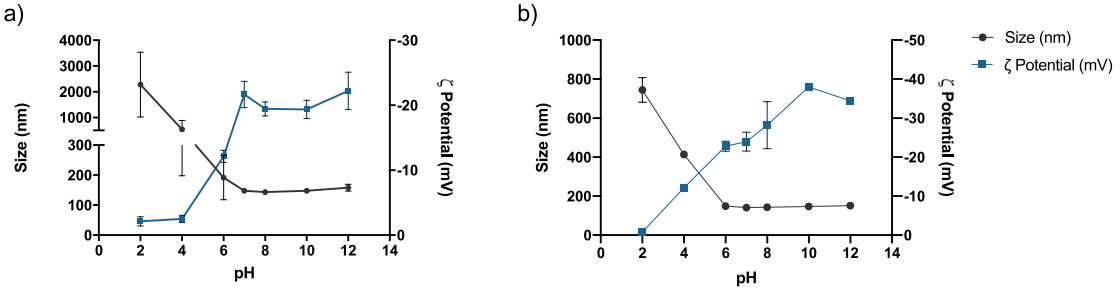

Fig. 5. Fluctuations in size and surface charge values of NLC along the studied pH interval. Graph a) represents the changes for NLC formulations in PBS, while Graph b) shows the changes for NLC formulations in Milli-Q® water.

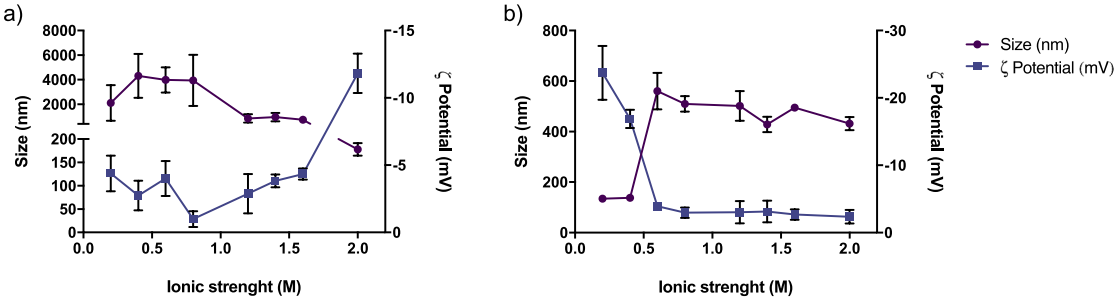

Fig. 6. Changes in size and surface charge values of NLC over the ionic strength predefined range. Graph a) represents the changes for NLC formulations in PBS, while Graph b) shows the changes for NLC formulations in Milli-Q® water.

media [88]. Fig. 6 shows the changes in size and surface charge of NLC formulations along the ionic strength range.

In the absence of additional NaCl salt and at a pH 7.4 value, lactoferrin-loaded NLC aqueous dispersions are stable systems, exhibiting no signal of caking or aggregation for, at least, 3 months (see section 4.3.1.). NLC stability is determined by electrostatic repulsive forces from the negative surface charge, being supported by previous studies [89,90]. Nevertheless, aggregation phenomena occurred in almost the entire studied ionic strength interval, possibly since NLC were just dispersed in PBS (pH 7.4 and 0.15 M ionic strength). A shift from a steady to an unsteady NLC formulation occurs for additional ionic strength values higher than 0.2 M and lower than 1.6 M, as presented in the Fig. 6a). A similar pattern was observed for the NLC formulations using Milli-Q® water instead of PBS for high ionic strength values (see Fig. 6b)), while for the 0.2 to 0.5 M range, the NLC size has remained unchanged, supporting the idea that PBS conditions such stability. Hence, an upsurge in the sodium ions concentration to the NLC colloidal suspension could compress the electric double layer weakened of nullified the magnitude of electrostatic repulsive influence, producing a noteworthy decrease of the ς potential. Consequently, a minimum increase in the ionic strength led to the coalescence of the NLC. In any case, the NLC suspension in the final formulation (PBS pH 7.4) presented suitable values of ionic strength and osmolarity for topical ophthalmic administration, without the need to add additional salts to the medium.

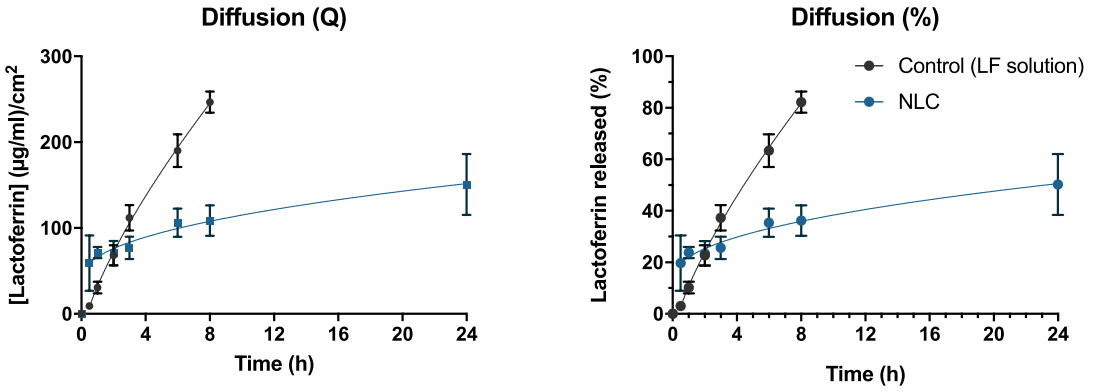

Fig. 7. *In vitro* release study of NLC, compared to a control solution. The first diagram illustrates the raw cumulative amount of Lf. The second diagram shows the cumulative percentage of Lf.

Table 3
Release data of NLC into the Higuchi and Peppas and Korsmeyer diffusion kinetics equation.

Formulation	Higuchi k ($mg \cdot cm^{-2} \cdot min^{-0.5}$)	R	Peppas and Korsmeyer k ($mg \cdot cm^{-2} \cdot min^{-n}$)	n	R
NLC	22.08	0.9754	26.67	0.45	0.9761

4.4. *In vitro release study*

Compared to the Lf buffered solution, the pilot *in vitro* release study from Lf-loaded NLC proved a controlled and maintained delivery behavior, as presented in Fig. 7. The *in vitro* Lf delivery profiles acquired for the NLC exhibited two dissimilar release stages caused by the nanocapsule structure and the different location of the Lf, adsorbed to the external lipid layer and immobilized into the polymeric gelled core. It can be observed: (I) a burst release due to the Lf desorption from the NLC surface, and (II) a sustained release due to the Lf diffusion across lipid layer from the NLC aqueous core.

Results from Lf cumulative release from NLC were adjusted to several kinetic models to find the pharmacokinetics and release behavior, where Higuchi and the Peppas and Korsmeyer kinetic models showed the best correlation data. In the latter model, a *n* value of 0.45 was obtained, advocating diffusion as the leading delivery mechanism (see details in Table 3). In absence of *in vivo* proteins with catalytic behavior (e.g., lipase, colipase), the main Lf delivery mechanism from the lipid NPs and NLC is assumed to be based on drug diffusion and lipid matrix erosion processes, but once the systems penetrate tissues, the *in vivo* lipid degradation by enzymes could be taken by increasing the intracellular release of the cargo. On the other hand, Robciuc et al. [91] (n) have previously described the presence of sphingolipid-specific enzymes, acid-and-neutral sphingomyelinases, as well as ceramidases in tears of healthy patients, forming part of the homeostatic system of the ocular surface. This enzymatic composition can be modified by the presence of bacterial lipases or extracellular stress. Thus, lipids and lipidic nanosystems can be altered on the ocular surface by the presence of enzymes, both in tear fluid or within the corneal epithelial cells and, therefore, the *in vivo* release could be faster.

4.5. *Ophthalmic toxicity analysis*

4.5.1. *Bovine corneal opacity and permeability test (BCOP)*

Corneal changes due to NLC administration were expressed as opacity and permeability values. Firstly, results were individually analyzed to assess whether NLC produce corneal irritation. No noteworthy variations were detected for NLC formulations, compared to the control solutions results (see Fig. 8). The IVIS score was finally obtained, where NLC showed a IVIS = 0, suggesting no corneal toxicity consequences compared to control formulations (see Fig. 9).

4.5.2. *Hen's egg test on the chorioallantoic membrane (HET-CAM)*

NLC formulations were assessed, comparing results with those acquired for the negative and positive control solutions (Fig. 10). NLC showed no cytotoxicity effects (IS = 0), being in accordance with the BCOP test results (see section 4.5.1.). Thus, resulting data confirmed that the constituents and the final lipidic formulations are non-toxic and biocompatible.

4.6. *Ocular surface retention study*

4.6.1. *Ex vivo ocular surface retention study*

Corneal mucin layer is a critical parameter that should be considered in the NLC design and development for ophthalmic delivery. The mucoadhesion variation for NLC formulations was expressed as the difference in the fluorescein concentration before and after the study.

Thus, a mucoadhesion percentage of 29.16 ± 6.54% and 47.23 ± 4.41% was obtained for the control solution and the NLC formulation,

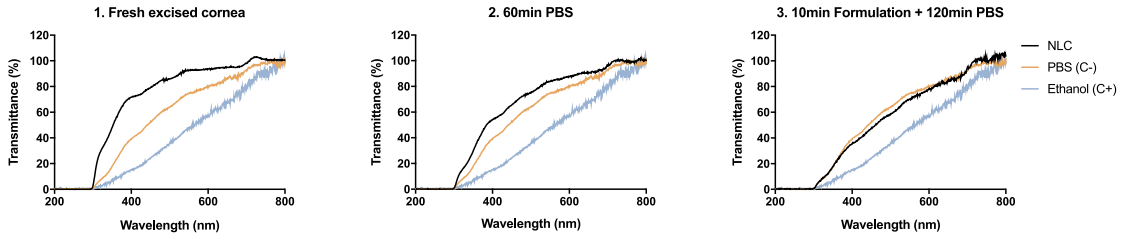

Fig. 8. Evolution of corneal transparency for NLC formulations over time during BCOP assay.

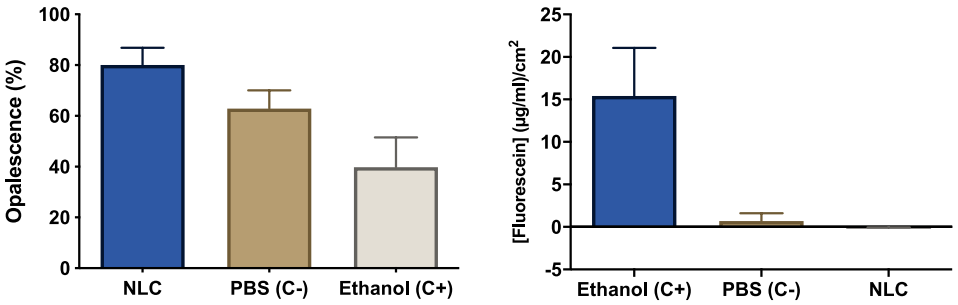

Fig. 9. Resulting data of opalescence and fluorescein permeability for NLC formulations, compared to control solutions, respectively.

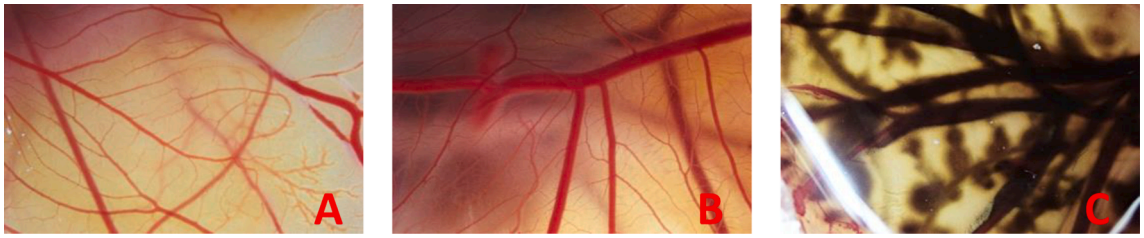

Fig. 10. Images of CAM membranes after the administration of NLC during the HET-CAM test, compared to the control solutions. (A) lactoferrin-loaded NLC, (B) NaCl aqueous solution (negative control), and (C) NaOH aqueous solution (positive control).

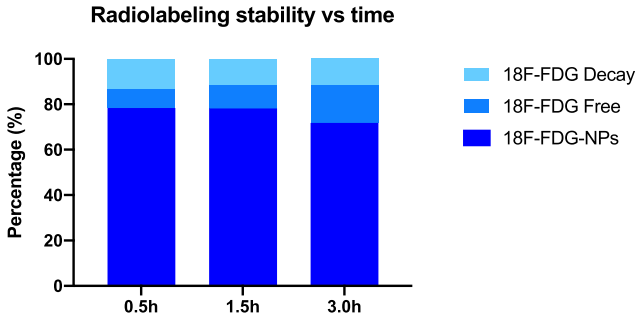

Fig. 11. ^{18}F-FDG radiolabeling efficiency and stability for NLCs over time.

respectively. Furthermore, a one-way ANOVA analysis was then performed, and statistically noteworthy differences ($p < 0.05$) were spotted by comparison of the results for NLCs with the standard data. This is in good agreement with previously published works [92,93], where NLC have proven a prolonged corneal MRT and a significant uptake along the corneal epithelium, conditioned by the small particle size and homogeneous particle size distribution.

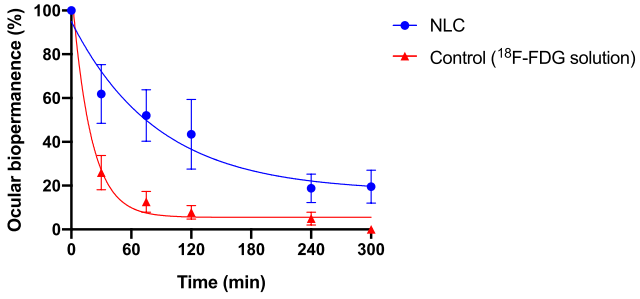

Fig. 12. Ocular biopermanence of a ^{18}F-FDG radiolabeled NLC and a ^{18}F-FDG aqueous solution (control), estimated considering the primary biopermanence data (%) in the ROI.

4.6.2. In vivo ocular surface retention study

4.6.2.1. Radiolabeling efficiency and stability of NLC. Fig. 11 displays the ^{18}F-FDG radiolabeling efficiency and stability for NLC formulations, respectively. As observed, ^{18}F-FDG NLC formulations presented an appropriate radiolabeling efficiency (higher than 75%) and stability for, at least, 3 h. ^{18}F-FDG was confirmed as a suitable radiotracer for NLC, and it was used in further *in vivo* radiolabeling assays.

4.6.2.2. Experimental in vivo evaluation of ocular biopermanence. Fig. 12 displays the ^{18}F-FDG-radiolabeled NLC ocular biopermanence for a 300-min period, compared to the standard solution. The corneal surface retention study of the NLC formulations was evaluated by the ^{18}F-FDG radioactivity assessment in a PET system.

The NLC ocular biopermanence was carried out on rats using ^{18}F-FDG as a radiotracer, trailed by the radioactivity evaluation in a PET equipment over the studied time (see details in Fig. 12). In this study, a higher MRT was detected for the NLCs, compared to the standard solution, even though both formulations consist of an ocular buffered solution (PBS, pH 7.4), whose composition is close to tears. Results were accurately adjusted to a monoexponential decline outline by a single compartmental model ($R = 0.9578$ for NLC and $R = 0.9930$ for the standard solution) (see Fig. 13). The resulting data are in good agreement with the idea that NLCs exhibit appropriate mucoadhesive, direct cell uptake, and corneal penetration, and according to the PET data of previous studies [94–96].

Table 4 displays the pharmacokinetics factors (k, $t_{1/2}$, MRT, AUC and R) of the ^{18}F-FDG radiolabeled NLC and ^{18}F-FDG standard solution. Statistically significant differences ($p < 0.05$) were spotted concerning NLC and control solution for the studied interval, where NLC showed a higher ocular retention profile.

The NLC ocular permanence obtained by PET was similar to that previously observed for the mucoadhesive Lf-loaded CS/TPP and CS/SBE-β-CD NPs [43]. Corneally, chitosan-based NPs showed a $t_{1/2}$ and MRT of 114 ± 72 h and 127 ± 47 h for CS/TPP NPs, and 60 ± 20 h and 90 ± 14 h for CS/SBE-β-CD NPs, respectively. Thus, results confirmed the great bioadhesive ability of the NLC in the ocular mucosa.

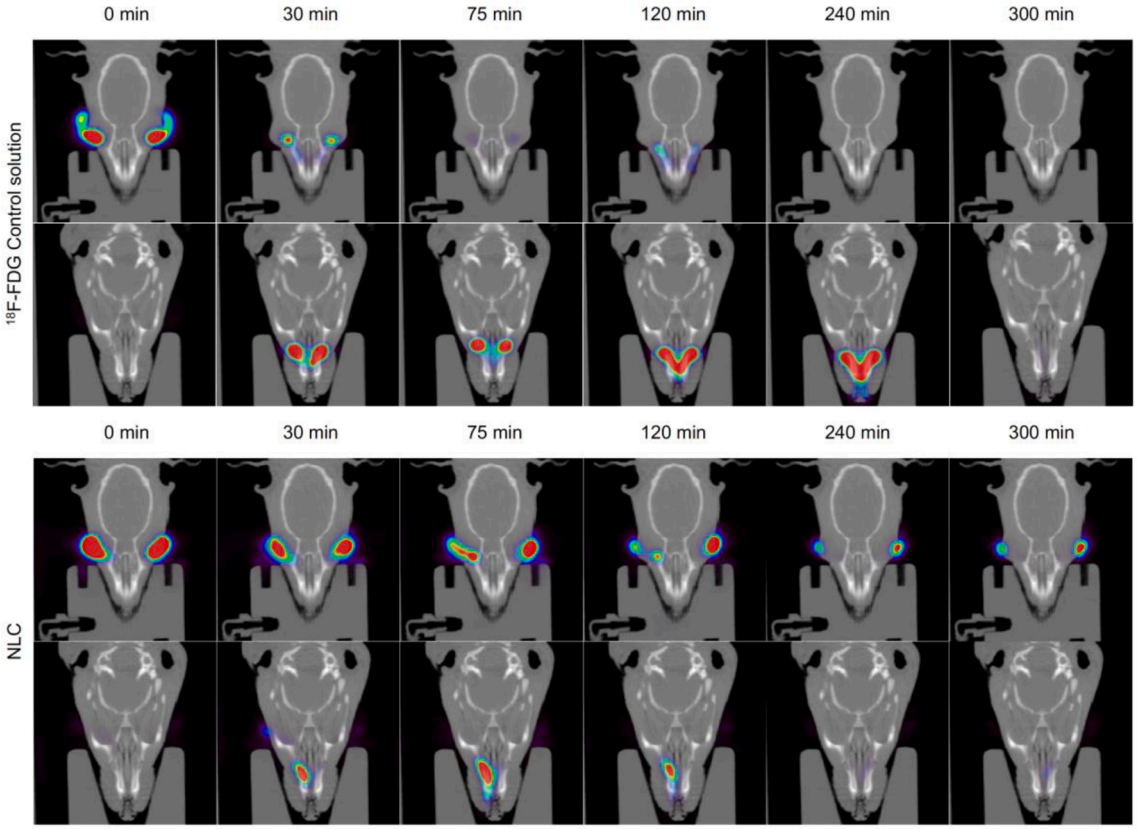

Fig. 13. Fused PET/CT images during the 5 h-studied interval. (I) ^{18}F-FDG buffered aqueous solution, (II) ^{18}F-FDG radiolabeled NLC.

Table 4
Ocular biopermanence parameters for ^{18}F-FDG radiolabeled NLC and ^{18}F-FDG control (named as "control" in the table) formulations.

Formulation	K (min^{-1})		$t_{1/2}$ (min)		MRT (min)		R^2	
	Mean	SD	Mean	SD	Mean	SD	Mean	SD
NLC	0.0071	0.0027	107.82	38.10	141.33	26.21	81.1	9.5
Control	0.041	0.012	17.7	4.5	59.1	17.6	26.0	7.8

5. Conclusion

In the biomedical field, nanoparticulate DDS have been extensively studied in the latest decades. Certainly, NLC have risen as a promising alternative to the conventional pharmaceutical forms in terms of the efficient delivery of therapeutics by different administration routes, including the topical ophthalmic pathway. Likewise, additional physicochemical properties of their excipients, such as high biocompatibility, biodegradability, and non-toxicity, support the use of NLC as new suitable DDS. The ease of scale, the controlled release profile, high stability and improved also reinforce the use of these novel nanosystems.

The elaboration of stable and tunable-size Lf-loaded NLC by double emulsion/solvent evaporation method is highly complex and is determined by different key process conditions, including the optimization of lipids concentration (both solid and liquid lipids), sonication and thermal shock conditions, among others.

In the present work, lactoferrin-loaded NLC showed an average particle size of 119.45 ± 11.44 nm, a 0.151 ± 0.045 nm PDI and a 17.50 ± 2.53 mV ç potential, as well as spherical and uniform shape. Similarly, these lipid nanosystems show good stability to storage (up to 3 months), to a 6–12 pH interval and to a 0.075–0.6 M ionic strength range in appropriate media. A controlled release of Lf was also proven, corroborating their use as possible DDS for hydrophilic drugs. Resulting data also confirmed their mucoadhesive properties through electrostatic forces for, at least, 240 min, with no evidence of tissue cytotoxicity.

To sum up, a NLC system was proposed for the first time for the topical ophthalmic delivery of lactoferrin, as an alternative to the present aggressive clinical approaches. Its design and development were reinforced by a consistent *in vitro* and *in vivo* characterization base. Similarly, NLC showed suitable physicochemical characteristics for ocular administration, delaying the drug release, and assuring the patient's adherence-to-treatment. Additionally, these lipid nanosystems versatility would permit their use in a huge variety of pharmaceutical forms for topical ophthalmic delivery.

Declaration of Competing Interest

The authors declare that they have no known competing financial interests or personal relationships that could have appeared to influence the work reported in this paper.

Acknowledgements

RVF and XGO acknowledge the financial support of the FIDIS (Health Research Institute of Santiago de Compostela Foundation). SEM and TEM analysis were feasible thanks to the Electronic and Confocal Microscopy Unit of the University of Santiago de Compostela (USC) (CACTUS, Spain). The work was partially supported by the Spanish Ministry of Science, Innovation and Universities (RTI2018-099597-B-100).

References

[1] R. Gaudana, H.K. Ananthula, A. Parenky, A.K. Mitra, Ocular Drug Delivery, AAPS J. 12 (3) (2010) 348–360, https://doi.org/10.1208/s12248-010-9183-3.
[2] R. Varela-Fernández, V. Díaz-Tomé, A. Luaces-Rodríguez, A. Conde-Penedo, X. García-Otero, A. Luzardo-Álvarez, A. Fernández-Ferreiro, F. Otero-Espinar, Drug Delivery to the Posterior Segment of the Eye: Biopharmaceutic and Pharmacokinetic Considerations, Pharmaceutics 12 (3) (2020) 269, https://doi.org/10.3390/pharmaceutics12030269.
[3] C. Le Bourlais, L. Acar, H. Zia, P.A. Sado, T. Needham, R. Leverge, Ophthalmic Drug Delivery Systems-Recent Advances, Prog. Retin. Eye Res. 17 (1) (1998) 33–58.
[4] A. Seyfoddin, J. Shaw, R. Al-Kassas, Solid Lipid Nanoparticles for Ocular Drug Delivery, Drug Deliv. 17 (7) (2010) 467–489, https://doi.org/10.3109/10717544.2010.483257.
[5] R.N. Saha, S. Vasanthakumar, G. Bende, M. Snehalatha, Nanoparticulate Drug Delivery Systems for Cancer Chemotherapy, Mol. Membr. Biol. 27 (7) (2010) 215–231, https://doi.org/10.3109/09687688.2010.510804.
[6] T. Tagami, T. Ozeki, Recent Trends in Clinical Trials Related to Carrier-Based Drugs, J. Pharm. Sci. 106 (9) (2017) 2219–2226, https://doi.org/10.1016/j.xphs.2017.02.026.
[7] C. Tapeinos, M. Battaglini, G. Ciofani, Advances in the Design of Solid Lipid Nanoparticles and Nanostructured Lipid Carriers for Targeting Brain Diseases, J. Control. Release Off. J. Control. Release Soc. 264 (2017) 306–332, https://doi.org/10.1016/j.jconrel.2017.08.033.
[8] N. Naseri, H. Valizadeh, P. Zakeri-Milani, Solid Lipid Nanoparticles and Nanostructured Lipid Carriers: Structure Preparation and Application, Adv. Pharm. Bull. 5 (2015) 305–313, https://doi.org/10.15171/apb.2015.043.
[9] A. Patel, K. Cholkar, V. Agrahari, A.K. Mitra, Ocular Drug Delivery Systems: An Overview, World J. Pharmacol. 2 (2013) 47–64, https://doi.org/10.5497/wjp.v2.i2.47.
[10] E. Sánchez-López, M. Espina, S. Doktorovova, E.B. Souto, M.L. García, Lipid Nanoparticles (SLN, NLC): Overcoming the Anatomical and Physiological Barriers of the Eye - Part II - Ocular Drug-Loaded Lipid Nanoparticles, Eur. J. Pharm. Biopharm. Off. J. Arbeitsgemeinschaft Pharm. Verfahrenstechnik EV 110 (2017) 58–69, https://doi.org/10.1016/j.ejpb.2016.10.013.
[11] D.-B. Chen, T.-Z. Yang, W.-L. Lu, Q. Zhang, In Vitro and in Vivo Study of Two Types of Long-Circulating Solid Lipid Nanoparticles Containing Paclitaxel, Chem. Pharm. Bull. (Tokyo) 49 (11) (2001) 1444–1447, https://doi.org/10.1248/cpb.49.1444.
[12] A. Fundarò, R. Cavalli, A. Bargoni, D. Vighetto, G.P. Zara, M.R. Gasco, Non-Stealth and Stealth Solid Lipid Nanoparticles (SLN) Carrying Doxorubicin: Pharmacokinetics and Tissue Distribution after i.v. Administration to Rats, Pharmacol. Res. 42 (4) (2000) 337–343, https://doi.org/10.1006/phrs.2000.0695.
[13] R.H. Müller, K. Mäder, S. Gohla, Solid Lipid Nanoparticles (SLN) for Controlled Drug Delivery - a Review of the State of the Art, Eur. J. Pharm. Biopharm. Off. J. Arbeitsgemeinschaft Pharm. Verfahrenstechnik EV 50 (2000) 161–177, https://doi.org/10.1016/s0939-6411(00)00087-4.
[14] A. Dingler, S. Gohla, Production of Solid Lipid Nanoparticles (SLN): Scaling up Feasibilities, J. Microencapsul. 19 (1) (2002) 11–16, https://doi.org/10.1080/02652040010018056.
[15] C. Freitas, R.H. Müller, Correlation between Long-Term Stability of Solid Lipid Nanoparticles (SLN) and Crystallinity of the Lipid Phase, Eur. J. Pharm. Biopharm. Off. J. Arbeitsgemeinschaft Pharm. Verfahrenstechnik EV 47 (2) (1999) 125–132.
[16] W. Mehnert, K. Mäder, Solid Lipid Nanoparticles: Production, Characterization and Applications, Adv. Drug Deliv. Rev. 47 (2001) 165–196, https://doi.org/10.1016/s0169-409x(01)00105-3.
[17] S.M. Kymes, J.J. Walline, K. Zadnik, J. Sterling, M.O. Gordon, Collaborative Longitudinal Evaluation of Keratoconus Study Group Changes in the Quality-of-Life of People with Keratoconus, Am. J. Ophthalmol. 145 (4) (2008) 611–617.e1, https://doi.org/10.1016/j.ajo.2007.11.017.
[18] M. Romero-Jiménez, J. Santodomingo-Rubido, J.S. Wolffsohn, Keratoconus: A review, Contact Lens and Anterior Eye J. Br. Contact Lens Assoc. 33 (4) (2010) 157–166.
[19] Z. Meiri, S. Keren, A. Rosenblatt, T. Sarig, L. Shenhav, D. Varssano, Efficacy of Corneal Collagen Cross-Linking for the Treatment of Keratoconus: A Systematic Review and Meta-Analysis, Cornea 35 (2016) 417–428, https://doi.org/10.1097/ICO.0000000000000723.
[20] R. Sharif, S. Bak-Nielsen, J. Hjortdal, D. Karamichos, Pathogenesis of Keratoconus: The Intriguing Therapeutic Potential of Prolactin-Inducible Protein, Prog. Retin. Eye Res. 67 (2018) 150–167, https://doi.org/10.1016/j.preteyeres.2018.05.002.
[21] I. Lema, J. Duran, Inflammatory Molecules in the Tears of Patients with Keratoconus, Ophthalmology 112 (4) (2005) 654–659, https://doi.org/10.1016/j.ophtha.2004.11.050.
[22] S.A. Balasubramanian, S. Mohan, D.C. Pye, M.D.P. Willcox, Proteases, Proteolysis and Inflammatory Molecules in the Tears of People with Keratoconus, Acta Ophthalmol. (Copenh.) 90 (2012) e303–309, https://doi.org/10.1111/j.1755-3768.2011.02369.x.
[23] I. Lema, D. Brea, R. Rodríguez-González, E. Díez-Feijoo, T. Sobrino, Proteomic Analysis of the Tear Film in Patients with Keratoconus, Mol. Vis. 16 (2010) 2055–2061.
[24] S.A. Balasubramanian, D.C. Pye, M.D.P. Willcox, Levels of Lactoferrin, Secretory IgA and Serum Albumin in the Tear Film of People with Keratoconus, Exp. Eye Res. 96 (1) (2012) 132–137, https://doi.org/10.1016/j.exer.2011.12.010.
[25] S.A. González-Chávez, S. Arévalo-Gallegos, Q. Rascón-Cruz, Lactoferrin: Structure, Function and Applications, Int. J. Antimicrob. Agents 33 (301) (2009) e1–301.e8, https://doi.org/10.1016/j.ijantimicag.2008.07.020.
[26] D. Legrand, A. Pierce, E. Elass, M. Carpentier, C. Mariller, J. Mazurier, Lactoferrin Structure and Functions, Adv. Exp. Med. Biol. 606 (2008) 163–194, https://doi.org/10.1007/978-0-387-74087-4_6.
[27] B.J. Appelmelk, Y.Q. An, M. Geerts, B.G. Thijs, H.A. de Boer, D.M. MacLaren, J. de Graaff, J.H. Nuijens, Lactoferrin Is a Lipid A-Binding Protein, Infect. Immun. 62 (1994) 2628–2632.
[28] K.-I. Hayashida, T. Kaneko, T. Takeuchi, H. Shimizu, K. Ando, E. Harada, Oral Administration of Lactoferrin Inhibits Inflammation and Nociception in Rat Adjuvant-Induced Arthritis, J. Vet. Med. Sci. 66 (2) (2004) 149–154, https://doi.org/10.1292/jvms.66.149.
[29] A.B. Schryvers, L.J. Morris, Identification and Characterization of the Human Lactoferrin-Binding Protein from Neisseria Meningitidis, Infect. Immun. 56 (1988) 1144–1149.
[30] R.T. Ellison, T.J. Giehl, Killing of Gram-Negative Bacteria by Lactoferrin and Lysozyme, J. Clin. Invest. 88 (1991) 1080–1091.
[31] N. Takakura, H. Wakabayashi, H. Ishibashi, S. Teraguchi, Y. Tamura, H. Yamaguchi, S. Abe, Oral Lactoferrin Treatment of Experimental Oral Candidiasis in Mice, Antimicrob. Agents Chemother. 47 (8) (2003) 2619–2623, https://doi.org/10.1128/AAC.47.8.2619-2623.2003.
[32] M. Marchetti, F. Superti, M.G. Ammendolia, P. Rossi, P. Valenti, L. Seganti, Inhibition of Poliovirus Type 1 Infection by Iron-, Manganese- and Zinc-Saturated Lactoferrin, Med. Microbiol. Immunol. (Berl.) 187 (4) (1999) 199–204, https://doi.org/10.1007/s004300050093.
[33] M.E. Murphy, H. Kariwa, T. Mizutani, H. Tanabe, K. Yoshimatsu, J. Arikawa, I. Takashima, Characterization of in Vitro and in Vivo Antiviral Activity of Lactoferrin and Ribavirin upon Hantavirus, J. Vet. Med. Sci. 63 (6) (2001) 637–645, https://doi.org/10.1292/jvms.63.637.
[34] B. Berkhout, R. Floris, I. Recio, S. Visser, The Antiviral Activity of the Milk Protein Lactoferrin against the Human Immunodeficiency Virus Type 1, Biometals 17 (2004) 291–294, https://doi.org/10.1023/B:BIOM.0000027707.82911.be.
[35] L.T. Eliassen, G. Berge, B. Sveinbjørnsson, J.S. Svendsen, L.H. Vorland, Ø. Rekdal, Evidence for a Direct Antitumor Mechanism of Action of Bovine Lactoferricin, Anticancer Res. 22 (2002) 2703–2710.
[36] H. Tsuda, K. Sekine, K.-I. Fujita, M. Iigo, Cancer Prevention by Bovine Lactoferrin and Underlying Mechanisms–a Review of Experimental and Clinical Studies, Biochem. Cell Biol. Biochim. Biol. Cell. 80 (1) (2002) 131–136, https://doi.org/10.1139/o01-239.
[37] J. Flanagan, M. Willcox, Role of Lactoferrin in the Tear Film, Biochimie 91 (1) (2009) 35–43, https://doi.org/10.1016/j.biochi.2008.07.007.
[38] U. Pattamatta, M. Willcox, F. Stapleton, N. Cole, Q. Garrett, Bovine Lactoferrin Stimulates Human Corneal Epithelial Alkali Wound Healing in Vitro, Invest. Ophthalmol. Vis. Sci. 50 (2009) 1636–1643, https://doi.org/10.1167/iovs.08-1882.
[39] S. Akira, K. Takeda, Toll-like Receptor Signalling, Nat. Rev. Immunol. 4 (7) (2004) 499–511, https://doi.org/10.1038/nri1391.
[40] T. Sobrino, U. Regueiro, M. Malfeito, A. Vieites-Prado, M. Pérez-Mato, F. Campos, I. Lema, Higher Expression of Toll-Like Receptors 2 and 4 in Blood Cells of Keratoconus Patiens, Sci. Rep. 7 (2017) 1–7, https://doi.org/10.1038/s41598-017-13525-7.
[41] M. Ueta, S. Kinoshita, Ocular Surface Inflammation Is Regulated by Innate Immunity, Prog. Retin. Eye Res. 31 (6) (2012) 551–575, https://doi.org/10.1016/j.preteyeres.2012.05.003.
[42] Gesto, M.I.L.; Sánchez, J.A.C.; MOREIRAS, T.S.; Perez, F.C. Biomarkers for Diagnosis and Prognosis of Corneal Ectatic Disorders 2016.
[43] R. Varela-Fernández, X. García-Otero, V. Díaz-Tomé, U. Regueiro, M. López-López, M. González-Barcia, M.I. Lema, F.J. Otero-Espinar, Design, Optimization, and Characterization of Lactoferrin-Loaded Chitosan/TPP and Chitosan/Sulfobutylether-β-Cyclodextrin Nanoparticles as a Pharmacological Alternative for Keratoconus Treatment, ACS Appl. Mater. Interfaces 13 (3) (2021) 3559–3575, https://doi.org/10.1021/acsami.0c18926.
[44] K. Jores, A. Haberland, S. Wartewig, K. Mäder, W. Mehnert, Solid Lipid Nanoparticles (SLN) and Oil-Loaded SLN Studied by Spectrofluorometry and Raman Spectroscopy, Pharm. Res. 22 (11) (2005) 1887–1897, https://doi.org/10.1007/s11095-005-7148-5.
[45] S.M. Moghimi, A.C. Hunter, T.L. Andresen, Factors Controlling Nanoparticle Pharmacokinetics: An Integrated Analysis and Perspective, Annu. Rev. Pharmacol. Toxicol. 52 (1) (2012) 481–503, https://doi.org/10.1146/annurev-pharmtox-010611-134623.

[46] N.P. Truong, M.R. Whittaker, C.W. Mak, T.P. Davis, The Importance of Nanoparticle Shape in Cancer Drug Delivery, Expert Opin. Drug Deliv. 12 (1) (2015) 129–142, https://doi.org/10.1517/17425247.2014.950564.
[47] A. Jithan, K. Madhavi, M. Madhavi, K. Prabhakar, Preparation and Characterization of Albumin Nanoparticles Encapsulating Curcumin Intended for the Treatment of Breast Cancer, Int. J. Pharm. Investig. 1 (2011) 119–125, https://doi.org/10.4103/2230-973X.82432.
[48] S. Selvamuthukumar, R. Velmurugan, Nanostructured Lipid Carriers: A Potential Drug Carrier for Cancer Chemotherapy, Lipids Health Dis. 11 (2012) 159, https://doi.org/10.1186/1476-511X-11-159.
[49] Q 1 A (R2) Stability Testing of New Drug Substances and Products. **2006**, 20.
[50] M.S. Muthu, S. Singh, Poly (D, L-Lactide) Nanosuspensions of Risperidone for Parenteral Delivery: Formulation and in-Vitro Evaluation, Curr. Drug Deliv. 6 (2009) 62–68, https://doi.org/10.2174/156720109787048302.
[51] P. Calvo, J.L. Vila-Jato, M.J. Alonso, Comparative in Vitro Evaluation of Several Colloidal Systems, Nanoparticles, Nanocapsules, and Nanoemulsions, as Ocular Drug Carriers, J. Pharm. Sci. 85 (1996) 530–536, https://doi.org/10.1021/js950474+.
[52] G.-P. Yan, R.-F. Zong, L. Li, T. Fu, F. Liu, X.-H. Yu, Anticancer Drug-Loaded Nanospheres Based on Biodegradable Amphiphilic ε-Caprolactone and Carbonate Copolymers, Pharm. Res. 27 (12) (2010) 2743–2752, https://doi.org/10.1007/s11095-010-0275-7.
[53] M. Chamberlain, S.C. Gad, P. Gautheron, M.K. Prinsen, IRAG Working Group 1. Organotypic Models for the Assessment/Prediction of Ocular Irritation. Interagency Regulatory Alternatives Group, Food Chem. Toxicol. Int. J. Publ. Br. Ind. Biol. Res. Assoc. 35 (1) (1997) 23–37.
[54] M. Balls, P.A. Botham, L.H. Bruner, H. Spielmann, The EC/HO International Validation Study on Alternatives to the Draize Eye Irritation Test, Toxicol. Vitro Int. J. Publ. Assoc. BIBRA 9 (6) (1995) 871–929, https://doi.org/10.1016/0887-2333(95)00092-5.
[55] M.S. Christian, R.M. Diener, Soaps and Detergents: Alternatives to Animal Eye Irritation Tests, J. Am. Coll. Toxicol. 15 (1) (1996) 1–44, https://doi.org/10.3109/10915819609008705.
[56] Loprieno, N. *Alternative Methodologies for the Safety Evaluation of Chemicals in the Cosmetic Industry*; CRC Press, 2019; ISBN 978-1-00-069678-3.
[57] J.F. Sina, P.D. Gautheron, A Multitest Approach to Evaluating Ocular Irritation in Vitro, Toxicol. Methods 4 (1) (1994) 41–49, https://doi.org/10.3109/15376519409049111.
[58] F.A. Barile, Validating and Troubleshooting Ocular In Vitro Toxicology Tests, J. Pharmacol. Toxicol. Methods 61 (2) (2010) 136–145, https://doi.org/10.1016/j.vascn.2010.01.001.
[59] B.M. Wagner, Book Review: Handbook of Toxicology, 2nd edition, Edited by Derelanko MJ and Hollinger MA, CRC Press, 1,414 pages, numerous tables and figures, 2001, Price $149.95, Toxicol Pathol 30 (4) (2002) 534.
[60] Salem, H.; Katz, S.A. *Alternative Toxicological Methods*; CRC Press, 2003; ISBN 978-0-203-00879-9.
[61] Eskes, C.; Bessou, S.; Bruner, L.; Curren, R.; Jones, P.; Kreiling, R.; Liebsch, M.; McNamee, P.; Pape, W.; Prinsen, M.K.; et al. Subgroup 3. Eye Irritation. 76.
[62] Sina, J.F.; Galer, D.M.; Sussman, R.G.; Gautheron, P.D.; Sargent, E.V.; Leong, B.; Shah, P.V.; Curren, R.D.; Miller, K. A Collaborative Evaluation of Seven Alternatives to the Draize Eye Irritation Test Using Pharmaceutical Intermediates. *Fundam. Appl. Toxicol.* **1995**, *26*, 20–31, doi:10.1006/faat.1995.1071.
[63] N.P. Luepke, Hen's Egg Chorioallantoic Membrane Test for Irritation Potential, Food Chem. Toxicol. Int. J. Publ. Br. Ind. Biol. Res. Assoc. 23 (2) (1985) 287–291, https://doi.org/10.1016/0278-6915(85)90030-4.
[64] S. Kalweit, R. Besoke, I. Gerner, H. Spielmann, A National Validation Project of Alternative Methods to the Draize Rabbit Eye Test, Toxicol. Vitro Int. J. Publ. Assoc. BIBRA 4 (4-5) (1990) 702–706.
[65] H. Spielmann, S. Kalweit, M. Liebsch, T. Wirnsberger, I. Gerner, E. Bertram-Neis, K. Krauser, R. Kreiling, H.G. Miltenburger, W. Pape, W. Steiling, Validation Study of Alternatives to the Draize Eye Irritation Test in Germany: Cytotoxicity Testing and HET-CAM Test with 136 Industrial Chemicals, Toxicol. Vitro Int. J. Publ. Assoc. BIBRA 7 (4) (1993) 505–510.
[66] V. Belgamwar, V. Shah, S.J. Surana, Formulation and Evaluation of Oral Mucoadhesive Multiparticulate System Containing Metoprolol Tartarate: An in Vitro-Ex Vivo Characterization, Curr. Drug Deliv. 6 (2009) 113–121, https://doi.org/10.2174/156720109787048285.
[67] K. Gradauer, C. Vonach, G. Leitinger, D. Kolb, E. Fröhlich, E. Roblegg, A. Bernkop-Schnürch, R. Prassl, Chemical Coupling of Thiolated Chitosan to Preformed Liposomes Improves Mucoadhesive Properties, Int. J. Nanomedicine 7 (2012) 2523–2534, https://doi.org/10.2147/IJN.S29980.
[68] S. Rojas, J.D. Gispert, S. Abad, M. Buaki-Sogo, V.M. Victor, H. Garcia, J.R. Herance, In Vivo Biodistribution of Amino-Functionalized Ceria Nanoparticles in Rats Using Positron Emission Tomography, Mol. Pharm. 9 (12) (2012) 3543–3550, https://doi.org/10.1021/mp300382n.
[69] C. Pérez-Campaña, V. Gómez-Vallejo, A. Martin, E.S. Sebastián, S.E. Moya, T. Reese, R.F. Ziolo, J. Llop, Tracing Nanoparticles in Vivo: A New General Synthesis of Positron Emitting Metal Oxide Nanoparticles by Proton Beam Activation, Analyst 137 (2012) 4902–4906, https://doi.org/10.1039/C2AN35863H.
[70] M. Allmeroth, D. Moderegger, B. Biesalski, K. Koynov, F. Rösch, O. Thews, R. Zentel, Modifying the Body Distribution of HPMA-Based Copolymers by Molecular Weight and Aggregate Formation, Biomacromolecules 12 (7) (2011) 2841–2849, https://doi.org/10.1021/bm2005774.
[71] M. Allmeroth, D. Moderegger, D. Gündel, H.-G. Buchholz, N. Mohr, K. Koynov, F. Rösch, O. Thews, R. Zentel, PEGylation of HPMA-Based Block Copolymers Enhances Tumor Accumulation in Vivo : A Quantitative Study Using Radiolabeling and Positron Emission Tomography, J. Controlled Release 172 (2013) 77–85, https://doi.org/10.1016/j.jconrel.2013.07.027.
[72] A. Fernández-Ferreiro, J. Silva-Rodríguez, F.J. Otero-Espinar, M. González-Barcia, M.J. Lamas, A. Ruibal, A. Luaces-Rodriguez, A. Vieites-Prado, T. Sobrino, M. Herranz, et al., Positron Emission Tomography for the Development and Characterization of Corneal Permanence of Ophthalmic Pharmaceutical Formulations, Invest. Ophthalmol. Vis. Sci. 58 (2017) 772–780, https://doi.org/10.1167/iovs.16-20766.
[73] The Association for Research in Vision and Ophthalmology- Statement for the Use of Animals in Ophthalmic and Vision Research Available online: https://www.arvo.org/About/policies/statement-for-the-use-of-animals-in-ophthalmic-and-vision-research/ (accessed on 22 July 2020).
[74] N. Burden, K. Aschberger, Q. Chaudhry, M.J.D. Clift, S.H. Doak, P. Fowler, H. Johnston, R. Landsiedel, J. Rowland, V. Stone, The 3Rs as a Framework to Support a 21st Century Approach for Nanosafety Assessment, Nano Today 12 (2017) 10–13, https://doi.org/10.1016/j.nantod.2016.06.007.
[75] Y. Zhang, M. Huo, J. Zhou, S. Xie, PKSolver: An Add-in Program for Pharmacokinetic and Pharmacodynamic Data Analysis in Microsoft Excel, Comput. Methods Programs Biomed. 99 (3) (2010) 306–314, https://doi.org/10.1016/j.cmpb.2010.01.007.
[76] M. García-Fuentes, D. Torres, M.J. Alonso, Design of Lipid Nanoparticles for the Oral Delivery of Hydrophilic Macromolecules, Colloids Surf. B Biointerfaces 27 (2-3) (2003) 159–168, https://doi.org/10.1016/S0927-7765(02)00053-X.
[77] A.J. Almeida, S. Runge, R.H. Müller, Peptide-Loaded Solid Lipid Nanoparticles (SLN): Influence of Production Parameters, Int. J. Pharm. 149 (2) (1997) 255–265, https://doi.org/10.1016/S0378-5173(97)04885-0.
[78] F. Cerreto, M. Scalzo, S. Cesa, P. Paolicelli, M.A. Casadei, Solid Lipid Nanosuspensions Based on Low Melting Lipids as Protective System of Retinyl Palmitate, J. Drug Deliv. Sci. Technol. 21 (6) (2011) 479–483, https://doi.org/10.1016/S1773-2247(11)50077-2.
[79] L.B. Jensen, E. Magnussson, L. Gunnarsson, C. Vermehren, H.M. Nielsen, K. Petersson, Corticosteroid Solubility and Lipid Polarity Control Release from Solid Lipid Nanoparticles, Int. J. Pharm. 390 (1) (2010) 53–60, https://doi.org/10.1016/j.ijpharm.2009.10.022.
[80] S. Doktorovová, J. Araújo, M.L. Garcia, E. Rakovský, E.B. Souto, Formulating Fluticasone Propionate in Novel PEG-Containing Nanostructured Lipid Carriers (PEG-NLC), Colloids Surf. B Biointerfaces 75 (2) (2010) 538–542, https://doi.org/10.1016/j.colsurfb.2009.09.033.
[81] J. Liu, Z. Qiu, S. Wang, L. Zhou, S. Zhang, A Modified Double-Emulsion Method for the Preparation of Daunorubicin-Loaded Polymeric Nanoparticle with Enhanced in Vitro Anti-Tumor Activity, Biomed. Mater. Bristol Engl. 5 (6) (2010) 065002, https://doi.org/10.1088/1748-6041/5/6/065002.
[82] S. Singh, A.K. Dobhal, A. Jain, J.K. Pandit, S. Chakraborty, Formulation and Evaluation of Solid Lipid Nanoparticles of a Water Soluble Drug: Zidovudine, Chem. Pharm. Bull. (Tokyo) 58 (5) (2010) 650–655, https://doi.org/10.1248/cpb.58.650.
[83] L. Hu, X. Tang, F. Cui, Solid Lipid Nanoparticles (SLNs) to Improve Oral Bioavailability of Poorly Soluble Drugs, J. Pharm. Pharmacol. 56 (2004) 1527–1535, https://doi.org/10.1211/0022357044959.
[84] Z. Huang, S. Hua, Y. Yang, J. Fang, Development and Evaluation of Lipid Nanoparticles for Camptothecin Delivery: A Comparison of Solid Lipid Nanoparticles, Nanostructured Lipid Carriers, and Lipid Emulsion, Acta Pharmacol. Sin. 29 (2008) 1094–1102, https://doi.org/10.1111/j.1745-7254.2008.00829.x.
[85] H. Bunjes, M.H.J. Koch, K. Westesen, Influence of Emulsifiers on the Crystallization of Solid Lipid Nanoparticles, J. Pharm. Sci. 92 (7) (2003) 1509–1520, https://doi.org/10.1002/jps.10413.
[86] H. Abdelkader, Z. Fathalla, H. Moharram, T.F.S. Ali, B. Pierscionek, Cyclodextrin Enhances Corneal Tolerability and Reduces Ocular Toxicity Caused by Diclofenac, Oxid. Med. Cell. Longev. 2018 (2018) 1–13, https://doi.org/10.1155/2018/5260976.
[87] Partheniades, E. Chapter 3 - Forces between Clay Particles and the Process of Flocculation. In *Cohesive Sediments in Open Channels*; Partheniades, E., Ed.; Butterworth-Heinemann: Boston, 2009; pp. 47–88 ISBN 978-1-85617-556-2.
[88] S. Sreekumar, F.M. Goycoolea, B.M. Moerschbacher, G.R. Rivera-Rodriguez, Parameters Influencing the Size of Chitosan-TPP Nano- and Microparticles, Sci. Rep. 8 (2018) 4695, https://doi.org/10.1038/s41598-018-23064-4.
[89] H. Jin, W. Zhou, J. Cao, S.D. Stoyanov, T.B.J. Blijdenstein, P.W.N. de Groot, L. N. Arnaudov, E.G. Pelan, Super Stable Foams Stabilized by Colloidal Ethyl Cellulose Particles, Soft Matter 8 (7) (2012) 2194–2205, https://doi.org/10.1039/C1SM06518A.
[90] N. Bizmark, M.A. Ioannidis, D.E. Henneke, Irreversible Adsorption-Driven Assembly of Nanoparticles at Fluid Interfaces Revealed by a Dynamic Surface Tension Probe, Langmuir ACS J. Surf. Colloids 30 (3) (2014) 710–717, https://doi.org/10.1021/la404357j.
[91] A. Robciuc, A.H. Rantamäki, M. Jauhiainen, J.M. Holopainen, Lipid-Modifying Enzymes in Human Tear Fluid and Corneal Epithelial Stress Response, Invest. Ophthalmol. Vis. Sci. 55 (2014) 16–24, https://doi.org/10.1167/iovs.13-12577.
[92] R. Liu, Z. Liu, C. Zhang, B. Zhang, Nanostructured Lipid Carriers as Novel Ophthalmic Delivery System for Mangiferin: Improving in Vivo Ocular Bioavailability, J. Pharm. Sci. 101 (10) (2012) 3833–3844, https://doi.org/10.1002/jps.23251.
[93] Q. Luo, J. Zhao, X. Zhang, W. Pan, Nanostructured Lipid Carrier (NLC) Coated with Chitosan Oligosaccharides and Its Potential Use in Ocular Drug Delivery System, Int. J. Pharm. 403 (1-2) (2011) 185–191, https://doi.org/10.1016/j.ijpharm.2010.10.013.

[94] A. Luaces-Rodríguez, R. Touriño-Peralba, I. Alonso-Rodríguez, X. García-Otero, M. González-Barcia, M.T. Rodríguez-Ares, L. Martínez-Pérez, P. Aguiar, N. Gómez-Lado, J. Silva-Rodríguez, M. Herranz, Á. Ruibal-Morell, M.J. Lamas, F.J. Otero-Espinar, A. Fernández-Ferreiro, Preclinical Characterization and Clinical Evaluation of Tacrolimus Eye Drops, Eur. J. Pharm. Sci. Off. J. Eur. Fed. Pharm. Sci. 120 (2018) 152–161.

[95] R. Mazet, X. García-Otero, L. Choisnard, D. Wouessidjewe, V. Verdoot, F. Bossard, V. Díaz-Tomé, V. Blanc-Marquis, F.-J. Otero-Espinar, A. Fernandez-Ferreiro, A. Gèze, Biopharmaceutical Assessment of Dexamethasone Acetate-Based Hydrogels Combining Hydroxypropyl Cyclodextrins and Polysaccharides for Ocular Delivery, Pharmaceutics 12 (8) (2020) 717, https://doi.org/10.3390/pharmaceutics12080717.

[96] I. Zaki, P. Fitzgerald, J.G. Hardy, C.G. Wilson, A Comparison of the Effect of Viscosity on the Precorneal Residence of Solutions in Rabbit and Man, J. Pharm. Pharmacol. 38 (1986) 463–466, https://doi.org/10.1111/j.2042-7158.1986.tb04611.x.